Transactions of the **13th International Conference on Structural Mechanics in Reactor Technology** (SMiRT 13), Escola de Engenharia - Universidade Federal do Rio Grande do Sul, Porto Alegre, Brazil, August 13-18, 1995

Crack initiation on 316L(N) CT specimens under fatigue and creep fatigue conditions

Laiarinandrasana, L.[1], Drubay, B.[1], Piques, R.[2], Laiarinandrasana, L.[2], Faidy, C.[3]
1) CEA/DRN/DMTSEMT/RDMS, CEN SACLAY, Gif sur Yvette, France
2) Centre des Matériaux - Ecole des Mines de Paris, Evry, France
3) EDF/SEPTEN, Villeubanne, France

1. INTRODUCTION

In power plants operating at elevated temperatures, components are subjected to a complex loading history including creep, fatigue or creep-fatigue effects. A practical engineering method for calculating crack initiation time for pre-existing defects is needed.

For this purpose, an important test program named AMORFIS has been performed at CEA Saclay. The aim is to study a methodology for prediction of crack initiation in 316L(N) austenitic stainless steel CT specimens at high temperature under pure creep and cyclic loadings with or without holdtime.

In this paper, we intend first, to show cyclic test results, including continuous fatigue with load and displacement control, creep-fatigue (load controlled at hold time) and fatigue-relaxation (displacement controlled at hold time). Secondly, interpretations of these tests are developed, based on crack initiation prediction.

2. TEST DESCRIPTION

AMORFIS test program uses a 316L(N) type austenitic stainless. Its chemical composition is shown in Table 1. The average grain size is about 50μm.

Thirty three crack initiation tests were performed (Tables 2-5) on normalized CT25 specimens at 600°C and 650°C. Specimen notches are machined with a tip radius of about 100μm. Load point displacement δ(N), where N is the current cycle number, is measured by using extensometer attached to the specimens. Crack length a(N) is monitored by DC potential drop technique. The number of cycle for initiation N_i is determined from a(N) data, as the cycle number necessary for the crack to grow over a critical distance d=50μm. Tests are stopped after about 200μm crack growth in order to focus the study on crack initiation. Fracture surfaces are examined with scanning electron microscopy for micromechanisms study purposes.

3. EXPERIMENTAL RESULTS

Plotting ($\Delta\delta=\delta_{max}-\delta_{min}$) or ($\Delta F=F_{max}-F_{min}$) versus N, for load or displacement control respectively, shows (Fig. 1) that these ranges remain constant during the initiation phase, ($N<N_i$). So, in a (ΔF, $\Delta\delta$) plot (Fig. 2), one point represents to one test. Furthermore, $\Delta\delta=C.\Delta F$ where C is the elastic compliance for CT specimens (Hudak and Saxena 1973).

In Fig. 3, crack growth rate da/dN versus Δa (crack growth) plot presents initially a plateau until 200-800μm depending on the ΔF value, then it decreases. Then, either crack arrests for low values of ΔF, or, da/dN increases again when ΔF is high enough. This behavior is related to fatigue short crack growth (K.J. Miller et al. 1986). At initiation, short crack ($\Delta a=50\mu m$) emanates from the initial notch (J.P. Polvora 1995).

As crack initiation was referred to $\Delta a = 50\mu m$, we are interested in the da/dN value in the plateau. Therefore, for one test corresponds one da/dN value.

4. INTERPRETATIONS

Even at 600°C and 650°C, elastic compliance relates ΔF versus $\Delta\delta$. Furthermore, cycle period and hold times (t_h=0.5h, 1h, 5h) are very short in comparison with transition time (H. Riedel 1981 - L. Laiarinandrasana 1994) for this material. So, ΔK parameter was chosen in order to characterize fatigue crack initiation. K is the stress intensity factor (ASTM E 399 1981) for CT specimen, and $\Delta K=K_{max}-K_{min}$. ΔK depends on both ΔF and crack length ratio a/W, which are constant during the initiation period.

4.1. Crack initiation prediction for continuous fatigue tests

During the initiation period ΔK and da/dN remain constant. Fig. 4 plots these parameters for all AMORFIS continuous fatigue tests (load and displacement control, at 600°C and 650°C). A Paris law at initiation, can be derived from Fig. 4 : $da/dN(m/cycle)=C.\Delta K^m$, where $C=7.3.10^{-11}$, $m\approx2.9$ were adjusted constants and ΔK MPa$\sqrt{m}$

ΔK range threshold $\Delta K_{th}\approx9$MPa$\sqrt{m}$ was deduced experimentally from CT37 and CT47 (see Table 2). C coefficient value is greater than usual for 316L(N) at 600°C and 650°C : short crack grows faster than long one. It was shown (J.P. Polvora 1995) that short cracks are not subjected to closure effects, so the above Paris law is likely an intrinsic one for 316L(N) steel at 600°C and 650°C.

Diagram does not depend neither on the loading control, nor on the 50°C variation of the temperature. K_{min} effects interfere only after the plateau, so it was not accounted for.

Prediction calculation can be done easily by integration of the Paris law. For a given value of the loading ΔK, crack growth rate da/dN can be calculated and it allows to deduce the number of cycles corresponding to a crack growth of about 50µm.

4.2. Crack initiation by fatigue loadings with hold time

When we plot da/dN versus ΔK curves for all AMORFIS tests with different hold times (Fig. 5). At 650°C and for a fixed value of ΔK, increasing the hold time t_h results in a crack growth rate da/dN increase for load controlled tests, whereas da/dN decreases for displacement controlled tests.

4.2.1. *Creep fatigue load controlled tests*

Assuming cyclic cumulative damage hypothesis as shown by R.P. Skelton (1993): $(1/N)_{creep\text{-}fatigue}=(1/N)_{fatigue}+D_{creep}$. (1).

Equation (1) leads to : $$\left(\frac{da}{dN}\right)_{creep-fatigue} = \frac{1}{\left(1 - D_{creep}N_{creep-fatigue}\right)^2}\left(\frac{da}{dN}\right)_{continuous\ fatigue} \quad (2)$$

which shows that there should be a shift between the Paris law and a creep-fatigue crack growth rate law. This shift is accounted for by an acceleration term where the creep damage appears. Fig. 5 shows that these shifts depend on the hold time values (0.5h-1h or 5h). First, we introduce the incremental creep damage law defined by R Piques (1989):

$$dD = A\Sigma^{\alpha}\varepsilon_{ceq}^{\beta}d\varepsilon_{ceq} \quad (3)$$

where : $A = 2.10^{-7}$, $\alpha = 2$, $\beta = -0.5$ are material constants at 600°C, Σ is the largest principal stress and ε_{ceq} is the equivalent creep strain at 50µm ahead of the crack tip. Creep crack initiation occurs when D reaches a critical value D_C ($0.03<D_C<0.06$) (R. Piques 1989 - Laiarinandrasana 1994).

Assuming that equation (3) describes creep damage evolution in the vicinity of the crack tip during a hold time, cyclic creep damage D_{creep} can be defined by :

$$D_{creep} = \int_{t=0}^{t_h} dD \Big/ \int_{t=0}^{T_i} dD \qquad (4)$$

Then, D_{creep} is a parameter which take the unity value when the crack initiation occurs. Now, we can calculate "experimental" values of D_{creep} (noted D^{exp}_{creep} with deduced values from equation (1) :

$$D^{exp}_{creep} = \frac{1}{N^i_{creep-fatigue}} - \frac{1}{N^i_{continuous\ fatigue}}$$

where $N^i_{creep-fatigue}$ indicates the experimental number of cycle at initiation by creep-fatigue and $N^i_{continuous\ fatigue}$ is the corresponding calculated value with Paris law

Fig. 6 compares calculated D_{creep} with D^{exp}_{creep} versus ΔK. D_{creep} was calculated with finite element results for Σ and ε_{ceq}, corresponding to actual AMORFIS pure creep tests (L. Laiarinandrasana 1994). Since pure creep tests need generally higher loads than cyclic one, points in Fig. 6 are not mixed in the same area. D_{creep} and D^{exp}_{creep} observe the same trend despite the usual creep large scatter band.

Prediction of crack initiation is then simple. Crack initiation occurs when the cumulative damage (by creep-fatigue) is equal to unity. Equation (1) is written like this :

$$(1 / N_{creep\text{-}fatigue}) = (1 / N_{fatigue}) + D_{creep}. \qquad (5)$$

Since the second member terms can be calculated at initiation by Paris law and with the incremental damage law, $N^i_{creep-fatigue}$ can be deduced from equation (5). However, this model is available for short hold time (up to 5h but less than creep transition time).

4.2.2. *Fatigue-relaxation displacement controlled tests*

For fatigue-relaxation tests (displacement controlled), da/dN decreases when t_h increases. At the same temperature and for the same ΔK level, this can be explained by the intensification of crack closure with the stress relaxation. But for tests carried out at 600°C with t_h = 5h, both points are located in the vicinity of Paris law line : hold time effect vanishes when t_h is high enough and when temperature is low enough. For engineering components it is usually the case. Therefore, the only knowledge of Paris law is sufficient to predict crack initiation time for assumed displacement controlled loadings.

5.CONCLUSION

In order to develop simplified methods to determine crack initiation times, an experimental test program has been performed at CEA Saclay on 316L(N) CT specimens at 600°C and 650°C under pure creep, cyclic loadings with or without hold time.

For continuous fatigue loadings, a Paris law has been established, at 600°C and 650°C, for load controlled and displacement controlled fatigue. Integration of this Paris law leads to a conventional crack initiation prediction.

A cumulative damage model is applied in order to interpret the increase of crack growth rate when cyclic loadings include dwell periods. Knowing Paris law and creep damage model at the working temperature, crack initiation prediction is possible.

For fatigue-relaxation tests, crack growth rate decreases when increasing the hold time. This phenomenon is related to the intensification of crack closure with the stress relaxation in the ligament. For larger hold times and at lower temperature, which are the case of many engineering components, the effects of hold time vanishes and the Paris law is expected to be sufficient for predicting crack initiation.

REFERENCES

ASTM E 399-81 (1981), Plane strain fracture toughness of metallic material

Hudak and Saxena (1973), The stress analysis of cracks handbook, Del Research Corporation.

Laiarinandrasana (1994), Crack initiation at high temperature on an austenitic stainless steel, Thesis, Ecole Nationale Supérieure des Mines de Paris.

Piques (1989), Mechanics and mechanisms to crack initiation and growth under viscoplastic conditions in an austenitic stainless steel, Thesis, Ecole Nationale Supérieure des Mines de Paris.

Polvora et al (1995), Short fatigue crack growth and closure behavior in an austenitic stainless steel at 600°C and 650°C, This conference (SMIRT 95)

Skelton (1993), Behaviour of defects at high temperatures, ESIS 15, Edited by R.A. Ainsworth and R.P. Skelton, Mechanical Engineering Publications London.

Riedel (1981), Creep deformation at crack tips in elastic viscoplastic solids, J. Mech. Phys. Solids, **29** : 35-49.

Table 1 : 316L(N) SA plate chemical composition (Wt. Pct.)

C	Ni	Cr	Mn	Si	Cu	S	P	Mo	Co	N2	B
0.02	12.2	17.51	1.76	0.35	0.13	0.004	0.021	2.35	0.11	0.071	0.0014

Table 2 : Continuous fatigue load controlled tests at 600°C and 650°C

Specimens	F_{max}/F_{min}(kN)	ΔF(kN)	a/W	θ(°C)	N_i(cycles)
CT26	11,3/0,3	11	0,55	650	68
CT18	11/1	10	0,55	650	73
CT27	9,3/0,3	9	0,55	650	126
CT28	7,3/0,3	7	0,55	650	204
CT36	6,3/0,3	6	0,55	650	264
CT37	5,3/0,3	5	0,55	650	88000
CT47	5,3/0,3	5	0,55	650	1406
CT42	7,3/0,3	7	0,55	600	157
CT46	9,8/0,2	9,6	0,55	600	153
CT61	11,3/0,3	11	0,55	600	65

Table 3 : Continuous fatigue displacement controlled tests at 600°C and 650°C

Specimens	$\delta_{max}/\delta_{min}$(mm)	Δδ(mm)	a/W	θ(°C)	N_i(cycles)
CT49	0,10/0,0	0,10	0,55	650	244
CT57	0,15/0,0	0,15	0,55	650	72
CT59	0,10/0,0	0,10	0,55	600	240
CT58	0,15/0,0	0,15	0,55	600	70

Table 4 : Creep-fatigue load controlled tests at 600°C and 650°C

Specimens	F_{max}/F_{min}(kN)	ΔF(kN)	a/W	t_h(h)	θ(°C)	N_i(cycles)
CT38	13,3/0,3	13	0,55	0,5	650	10
CT24	9,8/0,2	9,6	0,55	0,5	650	19
CT29	8,3/0,3	8	0,55	0,5	650	36
CT34	7,3/0,3	7	0,55	0,5	650	40
CT30	6,3/0,3	6	0,55	0,5	650	157
CT40	6,3/0,3	6	0,55	1,5	650	164
CT41	7,3/0,3	7	0,55	1,5	650	23
CT67	13,2/0,2	13	0,55	1,5	650	8
CT55	7,3/0,3	7	0,55	5	650	59
CT56	9,8/0,2	9,6	0,55	5	650	9
CT68	13,2/0,2	13	0,55	5	650	6
CT44	7,3/0,3	7	0,55	5	600	254
CT45	9,8/0,2	9,6	0,55	5	600	188

Table 5 : Fatigue-relaxation displacement controlled tests at 600°C and 650°C

Specimens	$\delta_{max}/\delta_{min}$(mm)	Δδ(mm)	a/W	t_h(h)	θ(°C)	N_i(cycles)
CT60	0,15/0,0	0,15	0,55	0,5	650	26
CT62	0,10/0,0	0,10	0,55	0,5	650	73
CT66	0,15/0,0	0,15	0,55	1,5	650	36
CT69	0,17/0,0	0,17	055	1,5	650	40
CT63	0,15/0,0	0,15	0,55	5	650	42
CT70	0,17/0,0	0,17	0,55	5	650	36

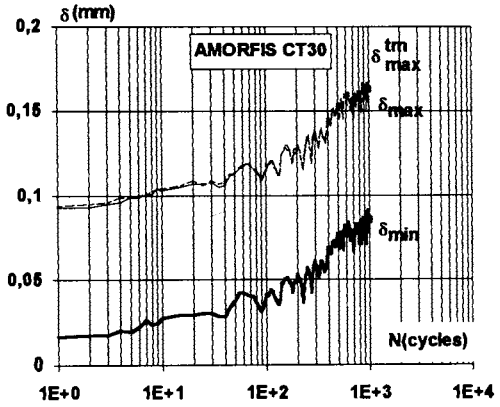

a/ Creep fatigue test CT30 (Load control)

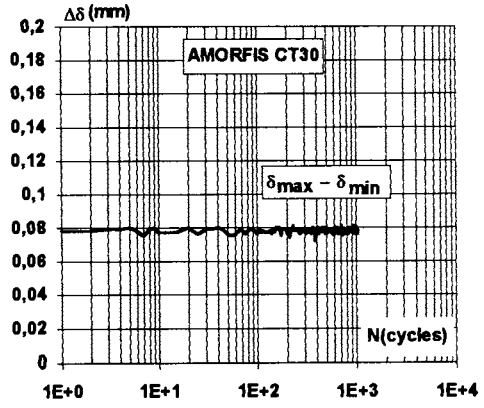

b/Creep fatigue test CT30 (Load control)

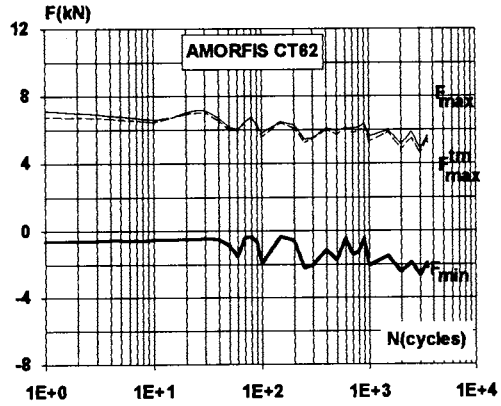

c/Fatigue-relaxation test CT62
(displacement control)

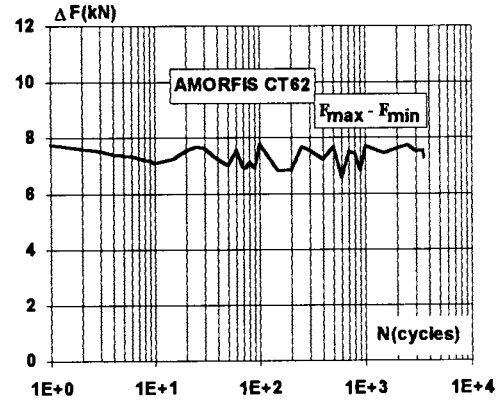

d/Fatigue-relaxation test CT62
(displacement control)

Figure 1

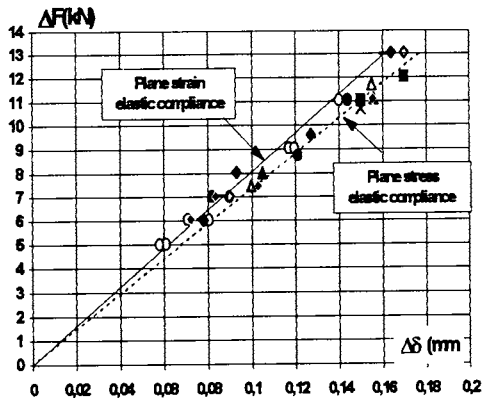

Figure 2
Elastic compliances comparison for cyclic loadings

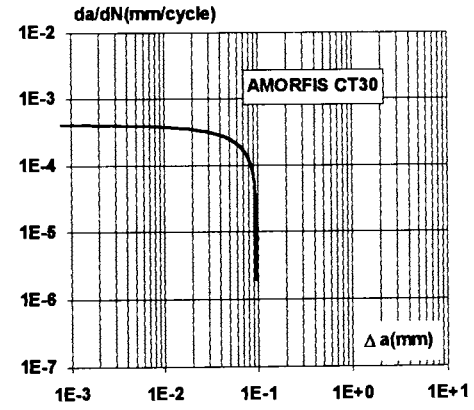

Figure 3
Crack growth rate evolution for CT30 specimen

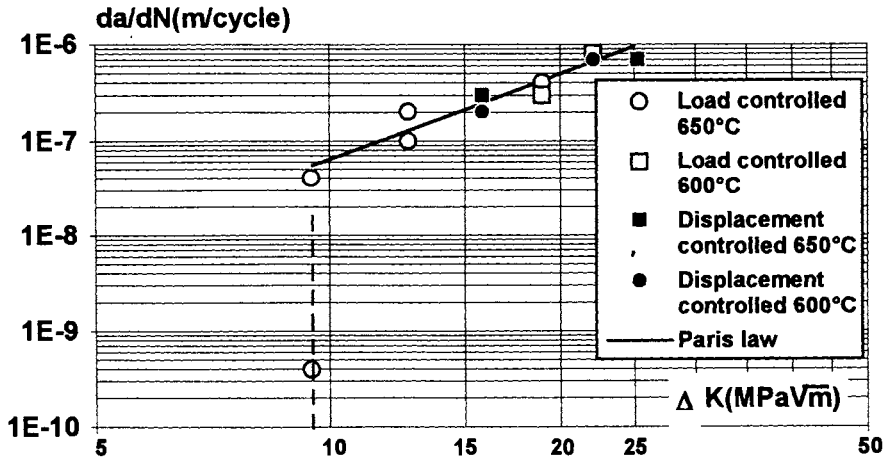

Figure 4 : Paris law at 650°C and 600°C

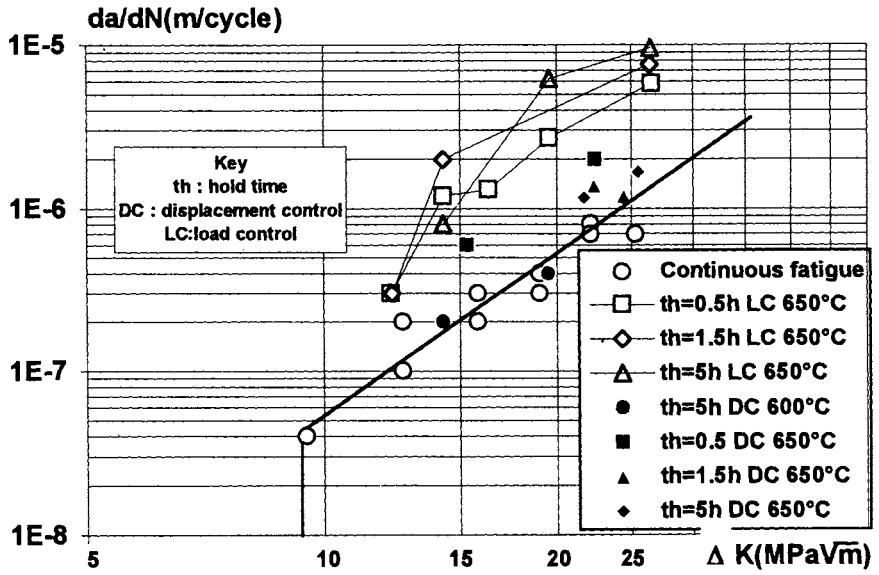

Figure 5 : Comparison between continuous fatigue Paris law and fatigue with hold time

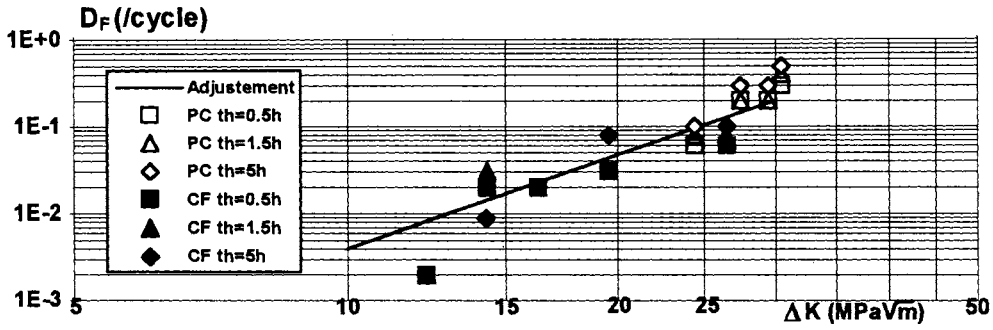

Figure 6 : Experimental values of D_F for creep-fatigue CF and calculated values for pure creep